

DIS structure functions and the double-spin asymmetry in ρ^0 electroproduction within a Regge approach

N. I. Kochelev^{ab1}, K. Lipka^{c2}, W.-D. Nowak^{c3}, V. Vento^{d4}, A. V. Vinnikov^{ae5}

^a BLTP, JINR, 141980, Dubna, Moscow region, Russia

^bInstitute of Physics and Technology, Almaty, 480082, Kazakhstan

^c DESY Zeuthen, 15738 Zeuthen, Germany

^d Departament de Física Teòrica and Institut de Física Corpuscular, Universitat de València-CSIC E-46100, Burjassot (Valencia), Spain

^e BK21 Physics Research Division, Seoul National University, Seoul, 151-742, Korea

Abstract

The proton, neutron and deuteron structure functions $F_2(x, Q^2)$ and $g_1(x, Q^2)$, measured at intermediate Q^2 , are analyzed within a Regge approach. This analysis serves to fix the parameters of this scheme which are then used to calculate, in a unified Regge approach, the properties of ρ^0 meson electroproduction on the proton and the deuteron. In this way, the double-spin asymmetry observed at HERMES in ρ^0 electroproduction on the proton, can be related to the anomalous behavior of the flavor-singlet part of the spin-dependent structure function $g_1(x, Q^2)$ at small x .

1 Introduction

Understanding the spin structure of the nucleon is today one of the main problems in hadron physics. Polarized beams have allowed significant progress in the measurement of the nucleon spin-dependent structure functions in the Deep Inelastic Scattering (DIS) regime. A result of some of these measurements [1] is that, at small values of Björken x , the neutron spin-dependent structure function $g_1^n(x, Q^2)$, which according to the $SU(6)_W$ model is dominated by the flavor singlet quark sea part, exhibits an anomalous behavior. More precisely, at $x \rightarrow 0$, $g_1^n(x, Q^2) \sim 1/x$, while the expected behavior should be $1/x^{\alpha_{a_1}}$, where a_1 is a conventional Regge trajectory with appropriate quantum numbers and intercept $\alpha_{a_1} = -0.5 \div 0.5$. Experimental data are thus well described in terms of a leading trajectory with an intercept close to 1, a value reminiscent of the Pomeron. In fact, this type of behavior at small x was predicted by leading order perturbative QCD calculations [2]. However, since next-to-leading order corrections to the perturbative BFKL Pomeron [3] are large [4], it is not clear to which extent the perturbative description is valid.

In Ref. [5], the observed anomalous behavior of $g_1^n(x, Q^2)$, was assumed to signal the existence of a flavor-singlet exchange with large intercept and negative signature, which was then used to explain the experimental data on diffractive hadronic reactions: vector meson photo-production at $\sqrt{s} \approx 100$ GeV, $|t|=1 \div 10$ GeV² and proton-proton elastic scattering at $\sqrt{s}=20 \div 60$ GeV, $|t|=2 \div 10$ GeV² [5], [6]. This exchange gives sizeable contributions to the differential

¹E-mail: kochelev@thsun1.jinr.ru

²E-mail: Katerina.Lipka@desy.de

³E-mail: Wolf.Dieter.Nowak@desy.de

⁴E-mail: Vicente.Vento@uv.es

⁵E-mail: vinnikov@thsun1.jinr.ru

cross-sections at large energy due to the large value of its intercept. We called it f_1 since its quantum numbers coincide with those of the axial vector $f_1(1285)$ meson ($P=C=+1$, negative signature). The mechanism leading to this exchange in QCD is not known. The relation of the Pomeron with the scale anomaly, led us to conjecture a relation between the f_1 and the gluonic axial anomaly, since the f_1 strongly mixes with gluonic degrees of freedom [5].

In order to investigate this unnatural-parity exchange the best observables are spin-dependent cross-sections. For example, we already have shown that the f_1 exchange leads to large double-spin asymmetries in different diffractive reactions [5], [7] and [8].

For s -channel helicity conserving (SCHC) reactions it seems reasonable, in the context of the VMD model, to establish a relation between the matrix elements describing the structure functions and vector meson electroproduction at low $-t$ (Fig.1). This relation arises naturally in the context of the Regge approach [9], where the imaginary part of the forward Compton scattering amplitude, relevant to describe DIS structure functions, and the total amplitude for vector meson production at $-t \rightarrow 0$ are connected.

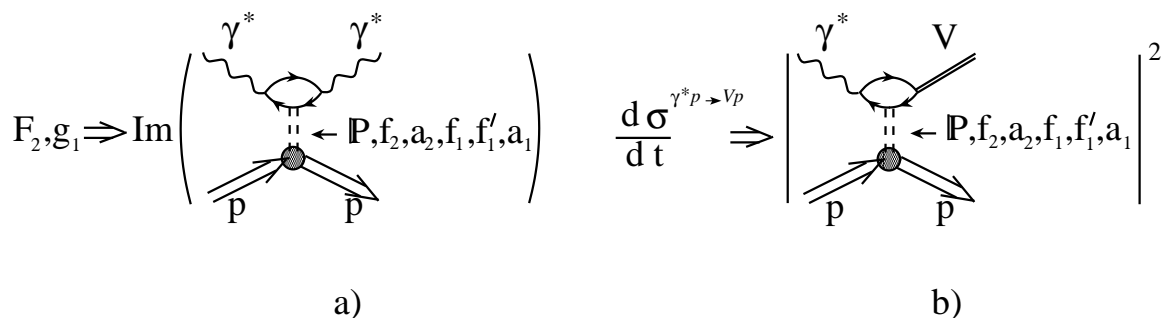


Figure 1: Within s -channel helicity conservation, the same exchanges describe both the structure functions F_2 and g_1 of inclusive deep inelastic lepton scattering [panel a)] and of vector meson production processes at high energy [panel b)].

The Regge model is a well known approach to describe diffractive reactions with small momentum transfer and high energy, a kinematical region where non-perturbative QCD effects are important. For this reason the investigation of diffraction and structure functions at low x are important items included into the experimental programs of the current and future accelerators: HERA, TEVATRON, RHIC, LHC, etc. These studies are expected to considerably enlarge the insight into the nature of strong interactions between quarks at large distances [10]. Several scenarios for the direct relation between the complex structure of the QCD vacuum and Regge behavior have been suggested [11], [12], [13].

The effective propagator for the spin-nonflip amplitude for scattering of two particles with momenta p_1 and p_2 has the following form in Regge theory:

$$D_R(s, t) = -\frac{1 + \sigma_R \cos(\pi\alpha_R(t)) - i \cdot \sigma_R \sin(\pi\alpha_R(t))}{\sin(\pi\alpha_R(t))\Gamma(\alpha_R(t))} \left(\frac{s}{s_0}\right)^{\alpha_R(t)-1}, \quad (1)$$

where $s = (p_1 + p_2)^2$, $t = (p_1 - p_2)^2$, s_0 is $\max(p_1^2, p_2^2, p_1'^2, p_2'^2)$, $\alpha_R(t)$ describes the Regge trajectory of the particles exchanged in the t channel and σ_R their signature, related to the spin J by $\sigma = (-1)^J$. The Γ function in the denominator provides the correct analytic behavior of the amplitude [14]. In many cases, a simpler formula can be used [15], but we prefer the original form in order to keep a precise relation between the real and the imaginary parts of the

amplitude. This relation will be used below to establish a connection between the properties of the DIS structure functions and those of vector meson electroproduction off the nucleon as suggested above.

Reggeons, with signature and space parities of the same sign, $\sigma = P$ (natural parity), have an amplitude which does not depend on the helicities of the colliding particles. Their exchange gives the dominant contributions to the spin-independent nucleon structure functions and to the total cross-sections. Exchanges with unnatural parity, $\sigma = -P$, have an amplitude which is proportional to the product of the particle helicities. Thus, only Reggeons with unnatural parities can contribute to the spin-dependent structure function $g_1(x, Q^2)$. Furthermore, a longitudinal double-spin asymmetry in two-particle scattering only arises when an unnatural-parity-exchange contribution to the scattering amplitude exists.

The main goal of this paper is an analysis of the deep-inelastic structure functions $F_2(x, Q^2)$ and $g_1(x, Q^2)$ in the framework of the Regge model; the extracted Reggeon parameters will be used to calculate the elastic cross-section, and finally the double-spin asymmetry, of ρ^0 electroproduction for intermediate values of Q^2 .

The Regge scheme will be defined by the exchange of trajectories with very large intercepts (Pomeron and the ‘anomalous’ component of f_1) and of secondary Regge trajectories, namely f_2 , a_2 , the ‘normal’ component of f_1 (which will be called f'_1) and a_1 . Especially the contributions of secondary Reggeons are considered to be of importance at HERMES energies.

2 The structure function $F_2(x, Q^2)$ in a Regge approach at intermediate values of Q^2

The parameters of the natural-parity Reggeons in soft interactions ($Q^2 < 1 \text{ GeV}^2$) are quite well known. They can be obtained from fits to the total hadronic cross-sections [16]. In particular, the parameters of the Pomeron, f_2 and a_2 Reggeon trajectories which are relevant for our calculation, are given by the Particle Data Group [17]:

$$\begin{aligned}\alpha_P(t) &= 1.093 + 0.25 t, & \beta_{Pqq} &= \beta_{PNN}/3 = 1.6 \text{ GeV}^{-1}, \\ \alpha_{f_2}(t) &= 0.358 + 0.9 t, & \beta_{f_2qq} &= \beta_{f_2NN}/3 = 4.7 \text{ GeV}^{-1}, \\ \alpha_{a_2}(t) &= 0.545 + 0.9 t, & \beta_{a_2qq} &= \beta_{a_2NN} = 4.91 \text{ GeV}^{-1},\end{aligned}\tag{2}$$

where β_{RNN} and β_{Rqq} are the coupling constants for the Reggeon-nucleon and Reggeon-quark couplings, respectively. The effective Lorentz structure of the coupling of these Reggeons to nucleons and quarks is assumed to be γ_μ [18]. The values of the slopes of the trajectories, which cannot be obtained from a fit to the total hadronic cross-sections, are taken from Ref. [9]. The relation between the couplings to quarks and nucleons is obtained from the naive constituent quark model. A clear separation of the secondary Reggeons and the Pomeron is possible because the energy dependences of their amplitudes described by the intercepts $\alpha(0)$, $\sigma_R^{tot} \sim s^{\alpha_R(0)-1}$ are very different. Specifically, the Pomeron contribution to the total hadronic cross-section rises as $s^{0.093}$, while, for example, the f_2 contribution falls as $s^{-0.642}$.

For large virtualities of the scattering particles, the effective intercepts of the Pomeron and the Reggeons change [19]. In particular, it was measured by the H1 and ZEUS Collaborations at HERA [20], [21] that the effective Pomeron intercept, extracted from the analysis of the $F_2(x, Q^2)$ structure function, ranges from ≈ 1.1 at $Q^2 \approx 0$ to ≈ 1.4 at $Q^2 > 10^2 \text{ GeV}^2$. Therefore, to make predictions for HERMES ($\langle Q^2 \rangle = 1.7 \text{ GeV}^2$), knowledge of the Pomeron and Reggeons intercepts at Q^2 values of a few GeV^2 is required.

The Regge formulae [22] for the proton and deuteron structure functions used are

$$\begin{aligned}
F_2^p(x, Q^2) &= \frac{Q^2}{Q^2 + \mu_N^2} \left(\frac{A_P}{x^{\alpha_P(0)-1}} + \frac{A_{f_2}}{x^{\alpha_{f_2}(0)-1}} + \frac{A_{a_2}}{x^{\alpha_{a_2}(0)-1}} \right), \\
F_2^d(x, Q^2) &= \frac{Q^2}{Q^2 + \mu_N^2} \left(\frac{A_P}{x^{\alpha_P(0)-1}} + \frac{A_{f_2}}{x^{\alpha_{f_2}(0)-1}} \right).
\end{aligned} \tag{3}$$

The various structure functions appearing in these equations represent the $SU(3)_f$ flavor singlet (the Pomeron), the $SU(2)_f$ isoscalar (f_2) and the isovector (a_2) exchanges. The parameter μ_N effectively accounts for the scaling violation at small Q^2 for the natural parity exchanges. Using Eq. (3) we made a fit to the recent data [23] at $Q^2 = 1 \div 3 \text{ GeV}^2$ and $x < 0.1$ (Regge region). The extracted parameters of Pomeron, f_2 and a_2 Reggeons are

$$\begin{aligned}
A_P &= 0.151, & \alpha_P(0) &= 1.206; \\
A_{f_2} &= 0.445, & \alpha_{f_2}(0) &= 0.64; \\
A_{a_2} &= 0.140, & \alpha_{a_2}(0) &= 0.33; \\
\mu_N &= 0.83 \text{ GeV}.
\end{aligned} \tag{4}$$

This fit provides a value of $\chi^2 = 192.8$ for 164 data points ($\chi^2/ndof=1.18$). It is evident that already in the semi-hard region (Q^2 -values of a few GeV^2) modified Regge intercepts have to be used. The slopes can be assumed to remain unchanged as they seem to vary quite slowly in this Q^2 region [24]. Moreover, they have no strong effect on the double-spin asymmetry.

3 The spin-dependent structure function $g_1(x, Q^2)$ in a Regge approach.

The parameters for the unnatural-parity Reggeons can be extracted from the data on the spin-dependent structure function $g_1(x, Q^2)$. We will use the relation between $g_1(x, Q^2)$ and the imaginary part of spin-dependent forward Compton scattering amplitude. By direct calculation (Fig.1a) the contribution of the unnatural-parity-Reggeon exchanges to this amplitude is obtained as:

$$T^{\mu\nu}(q, p, S) = \beta_{Rqq}\beta_{RNN}C_R\bar{u}(p, S)\gamma_\alpha\gamma_5u(p, S)R^{\mu\nu\alpha} \frac{1 - \exp\{-i\pi\alpha_R(0)\}}{\sin\{\pi\alpha_R(0)\}\Gamma(\alpha_R(0))} \left(\frac{2p \cdot q}{s_0}\right)^{\alpha_R(0)-1}, \tag{5}$$

where we assume that all exchanges f_1 , f_1' and a_1 have a $\gamma_\alpha\gamma_5$ Lorenz structure for both the quark and the nucleon vertices. The nucleon spin is denoted by S , and $s_0 \approx Q^2$ is the characteristic scale in the process.

The factor C_R is given by $e_u^2 + e_d^2 + e_s^2$ for the $SU(3)_f$ singlet ‘anomalous’ exchange (f_1), by $e_u^2 + e_d^2$ for the $SU(2)_f$ singlet ‘normal’ exchange (f_1') and by $e_u^2 - e_d^2$ for the $SU(2)_f$ triplet a_1 ; $R^{\mu\nu\alpha}$ is given by Ref. [25]

$$R^{\mu\nu\alpha} = -2 \int \frac{d^4k}{(2\pi)^4} \frac{\text{Tr}[(m_q + \hat{k} + \hat{q})\gamma^\nu(m_q + \hat{k})\gamma^\nu(m_q + \hat{k} + \hat{q})\gamma^\alpha\gamma_5]}{(k^2 - m_q^2)((k - q)^2 - m_q^2)}, \tag{6}$$

where $m_q \approx m_V/2$ is the mass of the quark in the quark loop in Fig.1.

Using the relation $\bar{u}(p, S)\gamma_\alpha\gamma_5u(p, S) = 2mS_\alpha$, and the formula

$$R^{\mu\nu\alpha} = \frac{1}{2\pi^2} q_\tau \epsilon^{\tau\mu\nu\alpha}, \tag{7}$$

for $-q^2 \gg m_q^2$ [26] we have

$$T^{\mu\nu}(q, p, S) = \frac{m}{\pi^2} C_R \beta_{Rqq} \beta_{RNN} S_\alpha q_\tau \epsilon^{\tau\mu\nu\alpha} \frac{1 - \exp\{-i\pi\alpha_R(0)\}}{\sin\{\pi\alpha_R(0)\} \Gamma(\alpha_R(0))} \left(\frac{2p \cdot q}{Q^2}\right)^{\alpha_R(0)-1}. \quad (8)$$

This expression is compared to the general form

$$T_{(spin)}^{\mu\nu} = i\epsilon^{\mu\nu\alpha\beta} q_\alpha S_\beta \frac{m}{pq} T_3 + i\epsilon^{\mu\nu\alpha\beta} q_\alpha (S_\beta(p \cdot q) - p_\beta(S \cdot q)) \frac{m}{(p \cdot q)^2} T_4, \quad (9)$$

where the DIS structure functions g_1 and g_2 are related to the amplitudes T_3, T_4 by

$$g_1(q, \nu) = -\frac{Im(T_3)}{2\pi}, \quad g_2(q, \nu) = -\frac{Im(T_4)}{2\pi}, \quad (10)$$

and where $\nu = p \cdot q$.

By assuming that g_2 structure function is small, we obtain

$$g_1(q, \nu) = \frac{\nu}{2\pi^3 \Gamma(\alpha_R(0))} C_R \beta_{Rqq} \beta_{RNN} \left(\frac{\nu}{Q^2}\right)^{\alpha_R(0)-1}. \quad (11)$$

Using $x = Q^2/(2\nu)$ we have

$$g_1(x, Q^2) = \frac{Q^2}{4\pi^3 \Gamma(\alpha_R(0))} (e_u^2 \pm e_d^2) C_R \beta_{Rqq} \beta_{RNN} \frac{1}{x^{\alpha_R(0)}}. \quad (12)$$

This form does not yet provide the correct scaling behavior for the structure function at $Q^2 \rightarrow \infty$ since the non-locality of the Reggeon-quark vertex in Fig.1a was not taken into account. Phenomenologically, this can be accomplished by introducing a form factor (similar as in the Pomeron case [27]):

$$F(Q^2) = \frac{\mu_U^2}{Q^2 + \mu_U^2}, \quad (13)$$

where μ_U is the effective parameter describing the scaling violation at low Q^2 for the unnatural-parity Reggeons. Then the contribution of a Reggeon to the $g_1(x, Q^2)$ structure function reads

$$g_1(x, Q^2) = \frac{\mu_U^2 C_R \beta_{Rqq} \beta_{RNN}}{4\pi^3 \Gamma(\alpha_R(0))} \frac{Q^2}{Q^2 + \mu_U^2} \frac{1}{x^{\alpha_R(0)}} \quad (14)$$

which provides the correct scaling behavior of the structure function at large Q^2 .

The parameters of the Reggeons with unnatural parity can be found from a fit to the available data on polarized DIS. Since data exist for proton, neutron and deuteron targets, this enables one to separate the isoscalar and isovector parts of the structure function. Using Eq. (14), the proton, neutron and deuteron structure functions can be presented as

$$g_1^p(x, Q^2) = g_1^{(1)}(x, Q^2) + g_1^{(3)}(x, Q^2), \quad (15)$$

$$g_1^n(x, Q^2) = g_1^{(1)}(x, Q^2) - g_1^{(3)}(x, Q^2), \quad (15)$$

$$g_1^d(x, Q^2) = g_1^{(1)}(x, Q^2), \quad (16)$$

where $g_1^{(1)}(x, Q^2)$ and $g_1^{(3)}(x, Q^2)$ are the isoscalar and isovector components, respectively.

It was pointed out [28] that the isoscalar part contains two components: ‘normal’ and ‘anomalous’. The ‘normal’ component has an intercept of $\alpha(0) \approx 0.5$ while the ‘anomalous’ has

a large intercept, $\alpha(0)$ close to 1. The isovector part contains only the ‘normal’ component. Thus the structure functions in Eq. (16) can be written as

$$g_1^{(1)}(x, Q^2) = \frac{2}{3} \frac{\mu_U^2 \beta_{f_1 qq} \beta_{f_1 NN}}{4\pi^3 \Gamma(\alpha_{f_1}(0))} \frac{Q^2}{Q^2 + \mu_U^2} \frac{1}{x^{\alpha_{f_1}(0)}} + \frac{5}{9} \frac{\mu_U^2 \beta_{f_1' qq} \beta_{f_1' NN}}{4\pi^3 \Gamma(\alpha_{f_1'}(0))} \frac{Q^2}{Q^2 + \mu_U^2} \frac{1}{x^{\alpha_{f_1'}(0)}}, \quad (17)$$

$$g_1^{(3)}(x, Q^2) = \frac{1}{3} \frac{\mu_U^2 \beta_{a_1 qq} \beta_{a_1 NN}}{4\pi^3 \Gamma(\alpha_{a_1}(0))} \frac{Q^2}{Q^2 + \mu_U^2} \frac{1}{x^{\alpha_{a_1}(0)}}. \quad (18)$$

For the fit we use the available data for $g_1(x, Q^2)$ [1] in the same kinematical region ($1 \text{ GeV}^2 < Q^2 < 3 \text{ GeV}^2$ and $x < 0.1$) which has been used above in fitting $F_2(x, Q^2)$. The resulting parameters are:

$$\alpha_{f_1}(0) = 0.938, \quad \beta_{f_1 qq} \beta_{f_1 NN} = -1.42 \text{ GeV}^{-2}; \quad (19)$$

$$\alpha_{f_1'}(0) = 0.412, \quad \beta_{f_1' qq} \beta_{f_1' NN} = 26.0 \text{ GeV}^{-2}; \quad (20)$$

$$\alpha_{a_1}(0) = 0.564, \quad \beta_{a_1 qq} \beta_{a_1 NN} = 36.2 \text{ GeV}^{-2}; \quad (21)$$

$$\mu_U = 1.161 \text{ GeV}, \quad (22)$$

which yield a χ^2 value of 35.9 for 58 data points (27 for g_1^p , 17 for g_1^n and 14 for g_1^d). We found that assuming different values of μ_U for the ‘anomalous’, isoscalar and isovector components does not provide a substantial improvement of the χ^2 value. Therefore we used the same μ_U for the three channels.

As before, it will be assumed that the slopes of the f_1' and a_1 exchanges are the same as the standard Reggeon value, i.e. 0.9 GeV^{-2} , while for the f_1 exchange we take the slope to be zero, as established in Ref. [5]. We mention again that the effect of the slopes on the double-spin asymmetry is negligible.

To check the quality of our approach to describe the $g_1(x, Q^2)$ structure functions, we calculate the Bjørken integral

$$I_{Bj} = \int_0^1 dx (g_1^p(x, Q^2) - g_1^n(x, Q^2)) \Big|_{Q^2 \rightarrow \infty} = \frac{g_A}{6} = 0.21, \quad (23)$$

within our model, resulting in

$$I_{Bj} = \int_0^1 dx \frac{\mu_U^2 \beta_{a_1 qq} \beta_{a_1 NN} (e_u^2 - e_d^2)}{2\pi^3 \Gamma(\alpha_{a_1}(0))} \frac{Q^2}{Q^2 + \mu_U^2} \frac{(1-x)^3}{x^{\alpha_{a_1}(0)}} \Big|_{Q^2 \rightarrow \infty} = 0.19. \quad (24)$$

In Eq. (24) an additional factor $(1-x)^3$ was introduced in order to describe the behavior of $g_1^{(3)}(x, Q^2)$ at $x \rightarrow 1$ according to the quark counting rules. Note that this factor has no significant influence on the low- x fit of $g_1(x, Q^2)$.

The comparison of Eqs. (23) and (24) leads to the conclusion that our model is in agreement with the Bjørken sum rule. This supports the expectation that it describes not only the structure functions F_2 and g_1 , but – in the context of SCHC – also vector meson production at small values of $-t$.

4 The cross-section of vector meson electroproduction

The cross-section of vector meson electroproduction reads (cf. Fig. 1b):

$$\frac{d\sigma}{d|t|} = \frac{|M(t)|^2}{64\pi W^2 (\vec{d}_{cm})^2}, \quad (25)$$

where $(\vec{q}_{cm})^2 = (W^4 + Q^4 + m_p^4 + 2W^2Q^2 - 2W^2m_p^2 + 2Q^2m_p^2)/4W^2$, W is center-of-mass energy of the virtual-photon proton system and m_p is the proton mass.

It was found [7],[27],[29] that the main features of the photoproduction reaction can be reproduced within a simple non-relativistic model for the vector meson wave function, where the quark and the anti-quark form the meson only if they have equal momenta. Above $Q^2 \approx 3 \text{ GeV}^2$, the quark's off-shellness and Fermi motion inside the vector meson have to be taken into account [30]. At smaller Q^2 these effects are not important and the non-relativistic model is applicable. In this framework, the Pomeron and f_2 Reggeon exchange amplitudes read [7]

$$\begin{aligned}
M_i &= 4m_V \beta_{Rqq} \beta_{RNN} \sqrt{\frac{3m_V \Gamma_{e^+e^-}}{\alpha_{em}}} \bar{u}(p_2) \gamma_\alpha u(p_1) \times \\
&\times \frac{(g_{\mu\nu} q^\alpha - g_{\nu\alpha} p_V^\mu - g_{\mu\alpha} q^\nu) \varepsilon_\gamma^\mu \varepsilon_V^\nu}{q^2 + t - m_V^2} \frac{1 + \exp\{-i\pi\alpha(t)\}}{\sin\{\pi\alpha(t)\} \Gamma(\alpha_R(t))} \left(\frac{s}{Q^2}\right)^{\alpha_R(t)-1} F_R^V(t) \approx \\
&\approx \frac{8m_V \beta_{Rqq} \beta_{RNN} Q^2}{Q^2 - t + m_V^2} \sqrt{\frac{3m_V \Gamma_{e^+e^-}}{\alpha_{em}}} \frac{1 + \exp\{-i\pi\alpha(t)\}}{\sin\{\pi\alpha(t)\} \Gamma(\alpha_R(t))} \left(\frac{s}{Q^2}\right)^{\alpha_R(t)} F_R^V(t),
\end{aligned} \tag{26}$$

where m_V is the mass of the vector meson and $\Gamma_{e^+e^-}$ is its leptonic width. The Regge parameters of the exchanges have been fixed above: $\beta_{Pqq} = \beta_{PNN}/3 = 1.6 \text{ GeV}^{-1}$, $\beta_{f_2qq} = \beta_{f_2NN}/3 = 4.7 \text{ GeV}^{-1}$, $\alpha_P(t) = 1.206 + 0.25 t$, $\alpha_{f_2}(t) = 0.64 + 0.9 t$.

The vector form factor of the Pomeron-NN vertex is [27]

$$F_P^V = \frac{4m_p^2 - 2.8 t}{(4m_p^2 - t)(1 - t/0.71)^2}. \tag{27}$$

We assume that the Pomeron and f_2 -Reggeon vertices have the same form factors. An additional factor has to be included to take into account the non-locality of these vertices,

$$\frac{\mu_N^2}{\mu_N^2 + Q^2 - t}, \tag{28}$$

where $\mu_N = 0.83 \text{ GeV}$ according to Eq. (4).

In a similar way one can obtain the unnatural-parity Reggeon contribution to the vector meson production amplitude [7].

$$\begin{aligned}
M_d &= 4m_V C'_R \beta_{Rqq} \beta_{RNN} \sqrt{\frac{3m_V \Gamma_{e^+e^-}}{\alpha_{em}}} \frac{\epsilon_{\mu\nu\alpha\beta} q^\beta \varepsilon_\gamma^\mu \varepsilon_V^\nu \bar{u}(p_2) \gamma_5 \gamma_\alpha u(p_1)}{q^2 + t - m_V^2} \times \\
&\times \frac{1 - \exp\{-i\pi\alpha_R(t)\}}{\sin\{\pi\alpha_R(t)\} \Gamma(\alpha_R(t))} \left(\frac{s}{Q^2}\right)^{\alpha_R(t)-1} \frac{\mu_U^2}{Q^2 + \mu_U^2} F_R^A(t) \approx \\
&\approx 8C'_R \lambda_\gamma \lambda_p m_V \beta_{Rqq} \beta_{RNN} \sqrt{\frac{3m_V \Gamma_{e^+e^-}}{\alpha_{em}}} \frac{Q^2}{Q^2 - t + m_V^2} \times \\
&\times \frac{1 - \exp\{-i\pi\alpha_R(t)\}}{\sin\{\pi\alpha_R(t)\} \Gamma(\alpha_R(t))} \left(\frac{s}{Q^2}\right)^{\alpha_R(t)} \frac{\mu_U^2}{Q^2 + \mu_U^2} F_R^A(t),
\end{aligned} \tag{29}$$

where λ_γ and λ_p are the helicities of the photon and the proton, respectively, and $C'_R = e_u - e_d$ for the 'anomalous' f_1 exchange and the 'normal' f_1' Reggeon, while $C''_R = e_u + e_d$. According to Eq. (22), the parameters of the exchanges are: $\alpha_{f_1}(t) = \alpha_{f_1}(0) = 0.938$, $\beta_{f_1qq} \beta_{f_1NN} = -1.42 \text{ GeV}^{-2}$, $\alpha_{f_1'}(t) = 0.412 + 0.9 t$, $\beta_{f_1'qq} \beta_{f_1'NN} = 26.0 \text{ GeV}^{-2}$, $\alpha_{a_1}(t) = 0.564 + 0.9 t$, $\beta_{a_1qq} \beta_{a_1NN} = 36.2 \text{ GeV}^{-2}$, $\mu_U = 1.161 \text{ GeV}$.

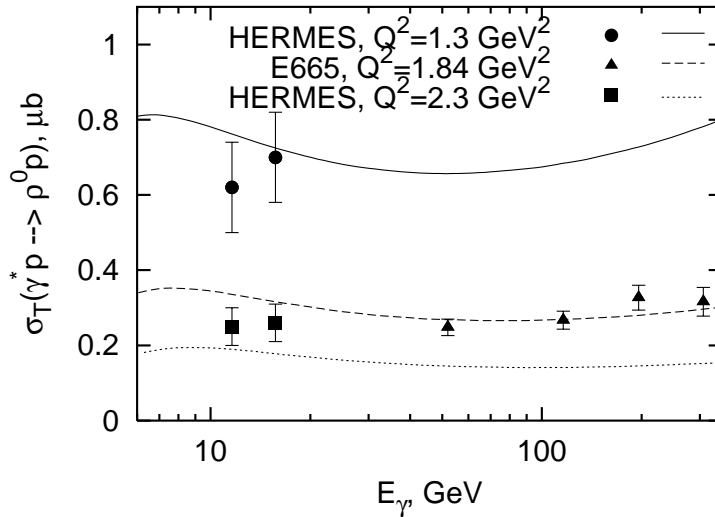


Figure 2: Cross-section of ρ^0 electroproduction by transverse photons. The data points shown here have been calculated from the published total and longitudinal cross-sections measured at HERMES [32] and at E665 [33]. The solid, dashed and dotted lines represent the model calculations at the given Q^2 values.

The axial vector form factor in the Reggeon-nucleon vertex is given by [31]

$$F_R^A(t) = \frac{1}{(1 - t/1.17)^2}. \quad (30)$$

Only the transverse cross-section of ρ^0 meson electroproduction is necessary to calculate double-spin asymmetries. As can be seen from Fig.2, the model described above is in fair agreement with experimental data [32],[33].

It is, however, necessary to verify whether the assumption of s -channel helicity conservation is valid for the description of ρ^0 electroproduction at HERMES. Otherwise, a large contribution from the spin-flip amplitude could exist which does not enter the matrix elements related to the structure functions and an important ingredient in the reaction mechanism could be lost. Experimentally [24] it was measured that SCHC violation is less than 10% .

5 The double-spin asymmetry in ρ^0 meson electroproduction

Recently, HERMES has published data on a sizeable double-spin asymmetry in ρ^0 meson electroproduction on the proton [34]. It is not expected that perturbative QCD calculations can explain this result, because for ρ^0 production at HERMES energy there is no hard scale available. In general, pQCD calculations based on two gluon-exchange in the t -channel predict a very small asymmetry at $t=0$ [35], [36]. The phenomenological Regge approach used here takes effectively into account non-perturbative effects of QCD which are important at HERMES energies.

The longitudinal double-spin asymmetry A_1^V for the interaction of transverse photons with a longitudinally polarized nucleon is defined as:

$$A_1^V(t) \equiv \frac{\sigma_T^{1/2} - \sigma_T^{3/2}}{\sigma_T^{1/2} + \sigma_T^{3/2}} = \frac{|M_T^{1/2}(t)|^2 - |M_T^{3/2}(t)|^2}{|M_T^{1/2}(t)|^2 + |M_T^{3/2}(t)|^2}. \quad (31)$$

Here $M_T^{1/2}$ and $M_T^{3/2}$ denote the transverse virtual photon scattering amplitudes where the superscript describes the projection of the total spin of the photon-nucleon system to the direction of the photon momentum. The amplitudes $M_T^{1/2,3/2}$ contain spin-independent parts made up by exchanges with natural parity ($M_N^{1/2,3/2}$) and spin-dependent parts made up by exchanges with unnatural parity ($M_U^{1/2,3/2}$). Between them the following relations hold

$$M_N^{1/2}(t) = M_N^{3/2}(t), \quad M_U^{1/2}(t) = -M_U^{3/2}(t). \quad (32)$$

Then

$$A_1^V(t) = \frac{2\text{Re}\{M_N^{1/2}(t)\}\text{Re}\{M_U^{1/2}(t)\} + 2\text{Im}\{M_N^{1/2}(t)\}\text{Im}\{M_U^{1/2}(t)\}}{|M_N^{1/2}(t)|^2 + |M_U^{1/2}(t)|^2}. \quad (33)$$

At this point this asymmetry can be analyzed qualitatively. Both types of amplitudes contain real and imaginary parts. The sign of the imaginary part can be determined using the optical theorem, the sign of the real part follows from the Regge formula given in Eq. (1). The optical theorem reads

$$\sigma_{tot} = \frac{1}{s}\text{Im}\{M(s, 0)\}. \quad (34)$$

Since the total cross-section of photon-nucleon scattering is positive, the imaginary parts of the forward photon-nucleon scattering amplitude for Pomeron and f_2 Reggeon exchanges are positive. It then follows from Eq. (1) that their real parts are negative. In the same way we deduce that the difference of imaginary parts of the photon-nucleon elastic scattering amplitude with anti-parallel and parallel spins $\Delta M_U = M_U^{1/2} - M_U^{3/2} = 2M_U^{1/2}$ is positive if the contribution of the corresponding exchange to the structure function $g_1(x, Q^2) \sim \sigma^{1/2} - \sigma^{3/2}$ is positive. The real part of ΔM_U in this case is also positive. If the contribution to the spin structure function $g_1(x, Q^2)$ is negative, the imaginary and real parts of the difference ΔM_U are negative.

It is worthwhile to note that a direct estimate of the vector meson production asymmetry based on the relation $A_1^V \approx 2A_1^{DIS}$ [37], even in the context of SCHC, does inherently not include the real part of the vector meson production amplitude as the DIS data on g_1 and F_2 are connected only to the imaginary part. For a full description, however, a way must be found to construct the real part which, in this paper, was chosen to be the Regge approach described above.

For the ‘anomalous’ f_1 exchange, the real part is much larger than the imaginary part and therefore this exchange should give a positive contribution to the asymmetry. For f_1' and a_1 exchanges, real and imaginary parts of the amplitudes contribute with different signs to the asymmetry. For scattering on the proton, their real parts give a negative asymmetry, and the imaginary parts give a positive one. This is also the case for f_1' exchange when scattering on the neutron and on the deuteron. For a_1 exchange in the case of scattering on the neutron, the real part of the amplitude leads to a positive double-spin asymmetry and the imaginary part leads to a negative one. Altogether, this discussion applies only to the region of small $|t|$ where the corresponding amplitudes do not change sign ($\alpha = 0$). Since the elastic cross-section originates mainly from the small $|t|$ region, we expect this qualitative analysis to be valid.

The result for the double-spin asymmetry on the proton is shown in e.g. Fig.3. It is evident that the contribution of the secondary f_1' and a_1 Reggeons to the asymmetry is not small. At HERMES energies, it is approximately the same as the contribution of the ‘anomalous’ f_1 exchange which we considered previously [7] within another approach.

More information about the flavor composition of the asymmetry can be obtained by measuring the asymmetry on deuteron and neutron. For the deuteron the isovector exchange contribution to A_1^V vanishes, and for the neutron it comes with the opposite sign and partly

cancels the regular isoscalar part. By this reason the ‘anomalous’ part can be observed best when studying data on the neutron.

In Figs. 3 - 8 the Regge-based predictions for the dependences of the double-spin asymmetry A_1^V on different kinematic variables are shown for both proton and deuteron. The predictions were calculated for the HERMES kinematics, $\langle W \rangle = 4.9$ GeV, $\langle Q^2 \rangle = 1.7$ GeV², $\langle x \rangle = 0.07$. The predictions are compared to measurements of ρ^0 electroproduction at HERMES [34, 38] on proton and deuteron. Although qualitative agreement can be seen only in the case of the proton, it is evident that experimental data with considerably improved precision are required.

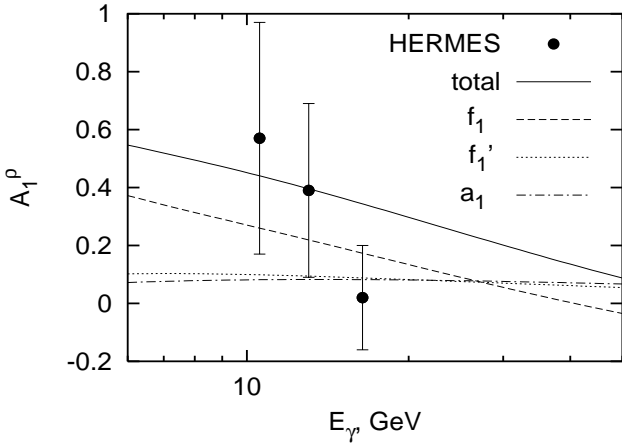


Figure 3: The E_{γ^*} -dependence of the double-spin asymmetry A_1^{ρ} on the proton, compared to data calculated from results of HERMES [34].

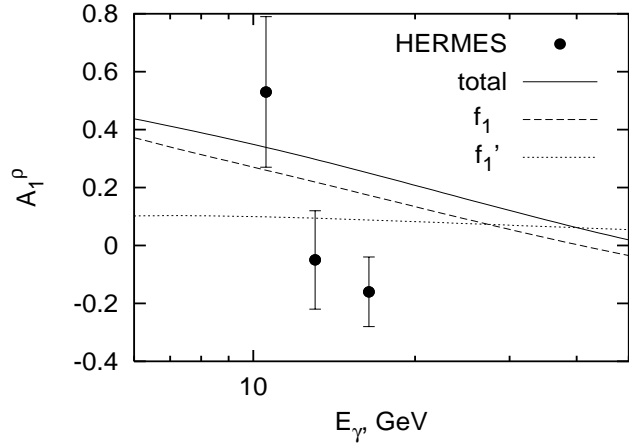


Figure 4: The E_{γ^*} -dependence of the double-spin asymmetry A_1^{ρ} on the deuteron, compared to data calculated from preliminary results of HERMES [38].

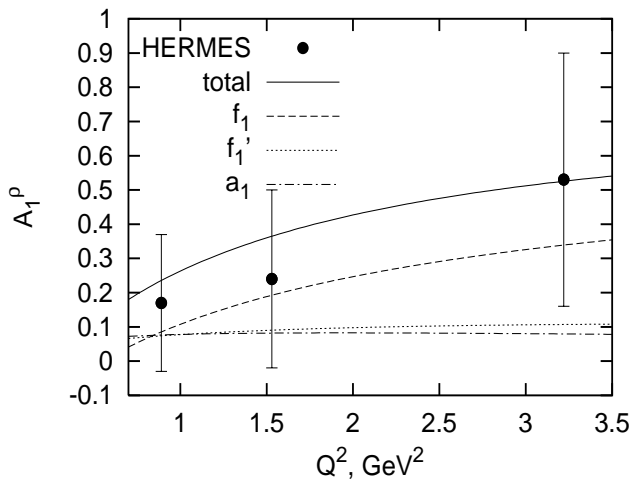


Figure 5: The Q^2 -dependence of the double-spin asymmetry A_1^{ρ} on the proton, compared to results of HERMES [34].

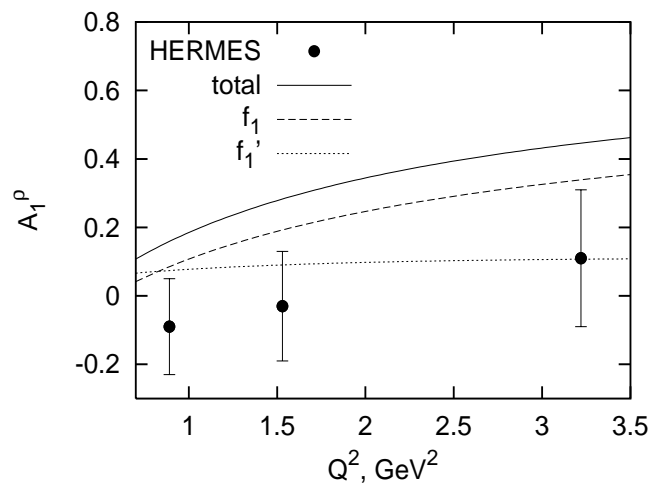


Figure 6: The Q^2 -dependence of the double-spin asymmetry A_1^{ρ} on the proton, compared to preliminary results of HERMES [38].

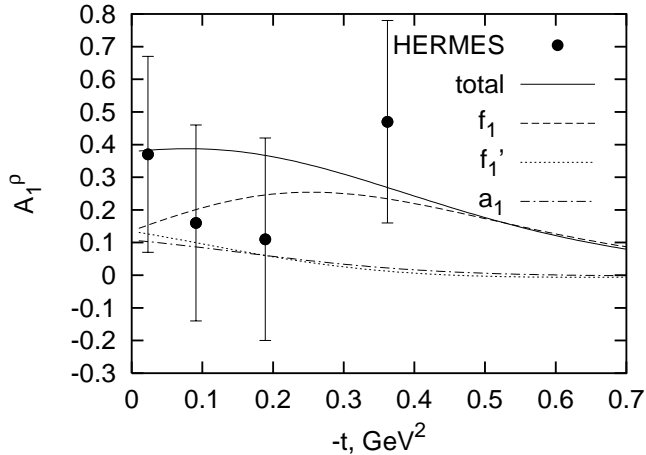


Figure 7: The $-t$ -dependence of the double-spin asymmetry A_1^p on the proton, compared to results of HERMES [34].

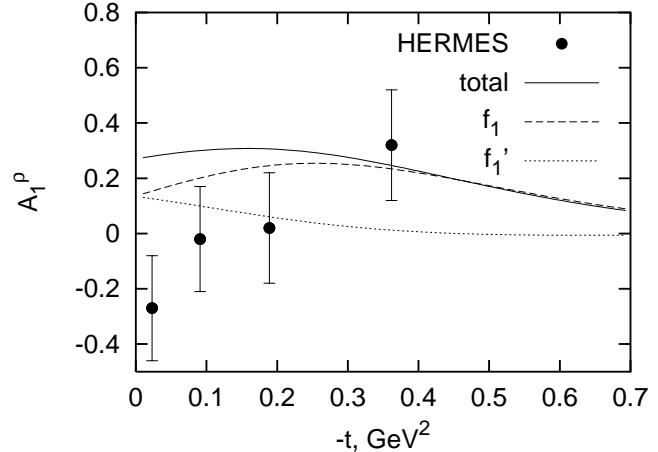


Figure 8: The $-t$ -dependence of the double-spin asymmetry A_1^p on the deuteron, compared to preliminary results of HERMES [38].

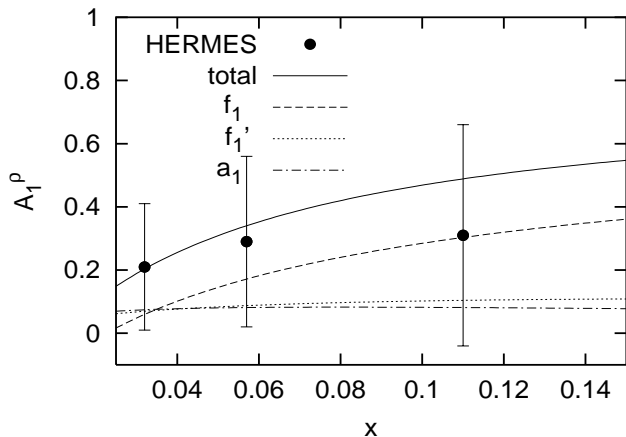


Figure 9: The x -dependence of the double-spin asymmetry A_1^p on the proton, compared to results of HERMES [34].

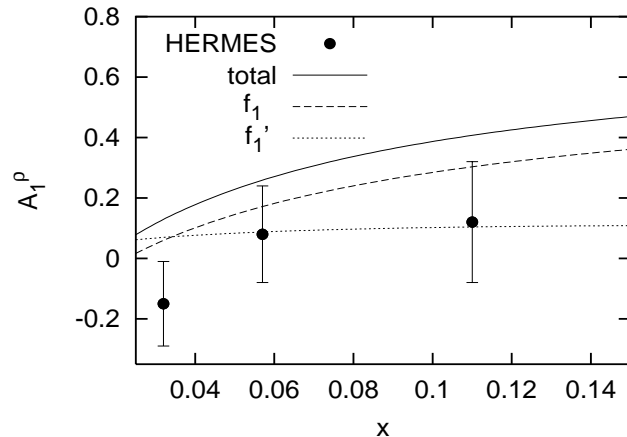


Figure 10: The x -dependence of the double-spin asymmetry A_1^p on the deuteron, compared to preliminary results of HERMES [38].

6 Conclusions

In summary, the nucleon structure functions $F_2(x, Q^2)$ and $g_1(x, Q^2)$ were analyzed in the framework of a Regge approach. From the data on deep inelastic scattering on the proton, neutron and deuteron we derived the parameters of Reggeons with natural and unnatural parities in the region $Q^2=1\div 3$ GeV². Using this parameterization and a non-relativistic model of ρ^0 meson formation which provides a fair description of the cross-section, we calculated the double-spin asymmetry of ρ^0 meson electroproduction at HERMES energies.

In this study we have used a unified approach to both DIS spin-dependent structure functions and vector meson electroproduction, in the context of s -channel helicity conservation. In this approach the obtained large value of the double-spin asymmetry in ρ^0 meson production is correlated with the anomalous behavior of the flavor-singlet part of the structure function $g_1(x, Q^2)$ at small x . In the case that future measurements will not confirm such a large asym-

metry, for a Regge-type analysis it would have to be concluded that the ‘anomalous’ f_1 exchange is not a simple Regge pole but has a more complicated structure, e.g. a Regge cut.

Acknowledgments

This work was supported by the following grants RFBR-01-02-16431, INTAS-2000-366, EC-IHP-HPRN-CT-2000-00130, MCyT-BFM2001-0262, GV01-216, and by the Heisenberg-Landau program. A.V. thanks ICTP for the warm hospitality extended to him during his stay when a part of this work was completed and V.V. acknowledges the hospitality of Seoul National University during the last stages of this work.

References

- [1] B. Adeva *et al.* [Spin Muon Collaboration], Phys. Rev. D **58**, 112001 (1998).
K. Abe *et al.* [E143 collaboration], Phys. Rev. D **58**, 112003 (1998).
A. Airapetian *et al.* [HERMES Collaboration], Phys. Lett. B **442**, 484 (1998).
P. L. Anthony *et al.* [E142 Collaboration], Phys. Rev. D **54**, 6620 (1996).
K. Abe *et al.* [E154 Collaboration], Phys. Rev. Lett. **79**, 26 (1997).
K. Ackerstaff *et al.* [HERMES Collaboration], Phys. Lett. B **404**, 383 (1997).
- [2] J. Bartels, B. I. Ermolaev and M. G. Ryskin, Z. Phys. C **72**, 627 (1996).
- [3] E. A. Kuraev, L. N. Lipatov and V. S. Fadin, Sov. Phys. JETP **45**, 199 (1977) [Zh. Eksp. Teor. Fiz. **72**, 377 (1977)].
- [4] V. S. Fadin and L. N. Lipatov, Phys. Lett. B **429**, 127 (1998).
- [5] N. I. Kochelev *et al.*, Phys. Rev. D **61**, 094008 (2000).
- [6] N. I. Kochelev *et al.*, Nucl. Phys. Proc. Suppl. **99A**, 24 (2001) [arXiv:hep-ph/0011042].
- [7] N. I. Kochelev, D. P. Min, V. Vento and A. V. Vinnikov, Phys. Rev. D **65**, 097504 (2002).
- [8] Y. Oh, N. I. Kochelev, D. P. Min, V. Vento and A. V. Vinnikov, Phys. Rev. D **62**, 017504 (2000).
- [9] P. D. Collins, “An Introduction To Regge Theory And High-Energy Physics,” *Cambridge 1977, 445p.*
- [10] E. Levin, TAUP-2465-97, DESY-97-213, arXiv:hep-ph/9710546.
- [11] A. B. Kaidalov and Y. A. Simonov, Phys. Lett. B **477**, 163 (2000).
- [12] D. Kharzeev and E. Levin, Nucl. Phys. B **578**, 351 (2000).
- [13] E. V. Shuryak and I. Zahed, Phys. Rev. D **62**, 085014 (2000).
- [14] M. Guidal, J. M. Laget and M. Vanderhaeghen, Nucl. Phys. A **627**, 645 (1997).
- [15] S. I. Manaenkov, arXiv:hep-ph/9903405.
- [16] A. Donnachie and P. V. Landshoff, Phys. Lett. B **296**, 227 (1992).

- [17] D. E. Groom *et al.* [Particle Data Group Collaboration], *Eur. Phys. J. C* **15**, 1 (2000).
- [18] P. V. Landshoff and O. Nachtmann, *Z. Phys. C* **35**, 405 (1987).
- [19] A. Capella, A. Kaidalov, C. Merino and J. Tran Thanh Van, *Phys. Lett. B* **343**, 403 (1995).
- [20] C. Adloff *et al.* [H1 Collaboration], *Phys. Lett. B* **520**, 183 (2001).
- [21] J. Breitweg *et al.* [ZEUS Collaboration], *Eur. Phys. J. C* **7**, 609 (1999).
- [22] H. Abramowicz, E. M. Levin, A. Levy and U. Maor, *Phys. Lett. B* **269**, 465 (1991).
A. Donnachie and P. V. Landshoff, *Z. Phys. C* **61**, 139 (1994).
- [23] M. R. Adams *et al.* [E665 Collaboration], *Phys. Rev. D* **54**, 3006 (1996).
M. Arneodo *et al.* [New Muon Collaboration], *Nucl. Phys. B* **483**, 3 (1997).
D. Allasia *et al.*, *Z. Phys. C* **28**, 321 (1985).
S. Aid *et al.* [H1 Collaboration], *Nucl. Phys. B* **470**, 3 (1996).
C. Adloff *et al.* [H1 Collaboration], *Nucl. Phys. B* **497**, 3 (1997).
M. Derrick *et al.* [ZEUS Collaboration], *Z. Phys. C* **69**, 607 (1996).
J. Breitweg *et al.* [ZEUS Collaboration], *Eur. Phys. J. C* **7**, 609 (1999).
- [24] M. Tytgat, DESY-THESIS-2001-018.
- [25] L. Rosenberg, *Phys. Rev.* **129**, 2786 (1963).
- [26] M. Anselmino, A. Efremov and E. Leader, *Phys. Rept.* **261**, 1 (1995) [Erratum-ibid. **281**, 399 (1997)].
- [27] A. Donnachie and P. V. Landshoff, *Phys. Lett. B* **185**, 403 (1987).
- [28] J. Soffer and O. V. Teryaev, *Phys. Rev. D* **56**, 1549 (1997).
S. D. Bass and M. M. Brisudova, *Eur. Phys. J. A* **4**, 251 (1999).
- [29] J. M. Laget, *Phys. Lett. B* **489**, 313 (2000).
- [30] I. Royen and J. R. Cudell, *Nucl. Phys. B* **545**, 505 (1999).
- [31] A. Liesenfeld *et al.* [A1 Collaboration], *Phys. Lett. B* **468**, 20 (1999).
- [32] A. Airapetian *et al.* [HERMES Collaboration], *Eur. Phys. J. C* **17**, 389 (2000).
- [33] M. R. Adams *et al.* [E665 Collaboration], *Z. Phys. C* **74**, 237 (1997).
- [34] A. Airapetian *et al.* [HERMES Collaboration], *Phys. Lett. B* **513**, 301 (2001).
- [35] M. Vanttinen and L. Mankiewicz, *Phys. Lett. B* **440**, 157 (1998),
M. Vanttinen and L. Mankiewicz, *Phys. Lett. B* **434**, 141 (1998).
- [36] S. V. Goloskokov, *Eur. Phys. J. C* **11**, 309 (1999).
- [37] H. Fraas, *Nucl. Phys. B* **113**, 532 (1976).
N. N. Nikolaev, *Nucl. Phys. Proc. Suppl.* **79**, 343 (1999).
- [38] K. Lipka (*for the HERMES Collaboration*), World Scientific, Proc. of PHOTON 2001, 186 (2002).